

MotionTrack: Learning Motion Predictor for Multiple Object Tracking

Changcheng Xiao, Qiong Cao, Yujie Zhong, Long Lan, Xiang Zhang, Huayue Cai, Zhigang Luo, Dacheng Tao, *Fellow, IEEE*.

Abstract—Significant advancements have been made in multi-object tracking (MOT) with the development of detection and re-identification (ReID) techniques. Despite these developments, the task of accurately tracking objects in scenarios with homogeneous appearance and heterogeneous motion remains challenging due to the insufficient discriminability of ReID features and the predominant use of linear motion models in MOT. In this context, we present a novel learnable motion predictor, named MotionTrack, which comprehensively incorporates two levels of granularity of motion features to enhance the modeling of temporal dynamics and facilitate accurate future motion prediction of individual objects. Specifically, the proposed approach adopts a self-attention mechanism to capture token-level information and a Dynamic MLP layer to model channel-level features. MotionTrack is a simple, online tracking approach. Our experimental results demonstrate that MotionTrack yields state-of-the-art performance on demanding datasets such as SportsMOT and Dancetrack, which feature highly nonlinear object motion. Notably, without fine-tuning on target datasets, MotionTrack also exhibits competitive performance on conventional benchmarks including MOT17 and MOT20.

Index Terms—multi-object tracking, motion modeling, Transformer, MLP.

I. INTRODUCTION

Multi-object tracking (MOT) has received more and more attention in recent years due to its promising applications in the fields [1]–[5] of intelligent surveillance, autonomous driving, mobile robotics, etc. Benefiting from the rapid development of object detection [6]–[10] and re-identification (ReID) [11]–[14], tracking-by-detection methods [15]–[18] have dominated. This paradigm consists of two main steps: 1) using an off-the-shelf object detector to obtain detection results for each frame, and 2) associating the detection results into trajectories using visual and motion cues. At association step, influenced by the inherent characteristics of the existing multi-object/pedestrian benchmarks [19], [20], most recent successes

Changecheng Xiao, Huayue Cai and Zhigang Luo are with College of Computer Science, National University of Defense Technology, Changsha 410073, China (email: xiaochangcheng16@nudt.edu.cn; huayue_cai@163.com; zglo@nudt.edu.cn).

Long Lan and Xiang Zhang are with Institute for Quantum Information & State Key Laboratory of High Performance Computing (HPCL), National University of Defense Technology, Changsha 410073, China (email: long.lan@nudt.edu.cn; zhangxiang08@nudt.edu.cn).

Qiong Cao and Dacheng Tao are with JD Explore Academy, Beijing 102628, China (email: mathqiong2012@gmail.com; dacheng.tao@gmail.com).

Yujie Zhong is with Meituan Inc., Beijing 100000, China (email: jaszhong@hotmail.com).

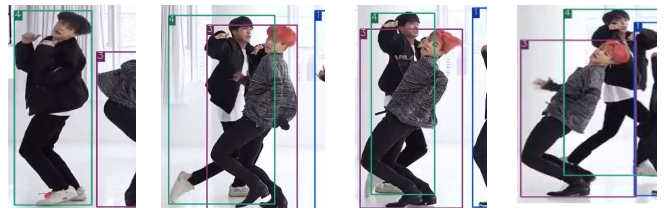
Corresponding author: Qiong Cao; Long Lan.



(a) SORT.



(b) OC_SORT



(c) MotionTrack

Fig. 1. Qualitative comparison of the proposed tracker with SORT and OC_SORT in a typical nonlinear motion scene. Samples obtained from frames 87, 126, 128 and 132 of video *Dancetrack0058*. When the dancer in black turns around and crosses paths with the red-haired dancer, the first two trackers emerge ID switch, and ours successfully tracks on.

on MOT [13], [14], [21] are based on either the appearance features or a junction of detection and simple tracking mechanism, leaving motion information under-explored. This trend makes existing trackers fail in situations [22], [23] where objects of interest share very similar appearance in group dancing and players possess rapid motion in sports scenes. It inspires us to take motion cues into modeling, which is critical to associate detection results accurately and efficiently.

In this work, we focus on learning a motion predictor to boost the accuracy of association and thus the performance

of tracking. It is very challenging due to complex motion variations across different scenarios and severe occlusions. The motion models used by existing trackers can be divided into classical algorithms based on Bayesian estimation [11], [14], [24]–[26] and data-driven algorithms [27]–[30]. For the former, a representative is Kalman filter [31]. It assumes constant velocity and thus works well with linear motion, but tends to fail in handling nonlinear motion. For the latter, the optical flow-based tracking method [27] requires a complex and heavy optical flow model to calculate the inter-frame pixel offsets, which can only consider local motion information and is limited by the time-consuming optical flow model [28]. Moreover, Long Short-Term Memory (LSTM) networks based methods [29], [32] are proposed to capture the inherent sequential motion by their latent space. However, LSTMs have been criticised by their memory mechanism [33] and capability of modeling temporal interaction [34].

In this study, we aim to address the aforementioned challenges and develop a data-driven motion predictor that is both simple and robust to complex temporal dependency and motion variations. We propose the use of Transformer networks, which have shown promising results in learning non-linear patterns, especially when large amounts of data are available. We believe that these networks are most suitable for modeling motion in multiple object tracking. We make the following contributions.

Firstly, we propose to use the powerful long-range dependency modeling capability of Transformer [35] to model the historical dynamics of an individual object to predict its motion. We can perform parallel computation of all objects and benefit from GPU acceleration. Furthermore, we study the behavioral influence of one object on others, and consider a joint modeling of the temporal and social interactions among objects. Experimental results (Tab. IX) show that such extension performs worse than the simple temporal interaction modeling without any complex social interaction terms. We surmise that this is because most of the scenes in Dancetrack are group dances where the dancers’ movements are pre-designed by the choreographer, making it challenging to learn the patterns of interaction between the dancers.

Secondly, as is commonly recognized, in the feature space, different semantic information tends to be distributed across distinct channels [36], [37]. Inspired by this, we endeavor to design a more powerful attention module to advance complex motion modeling to capture the information distributed over different channels (e.g. relative position change and direction of object motion). Specifically, we introduce a Multi-Layer Perceptron-like architecture named Dynamic MLP to explore motion information distributed in different channels precisely in the non-local range with content-adaptive token-mixing. With dynamic MLP, we further integrate it with the self-attention module in Transformer [35] to enable message passing at two different granularities, i.e., token level and channel level, for the purpose of aggregating different semantic messages. Moreover, we obtain complex motion patterns via different data augmentations to better understand motion dynamics and boost the tracking performance. Specifically, random drop, random spatial jitter and random length are

adopted to create motions with fast-moving objects, tracklets of different lengths, etc.

Our proposed method, although straightforward, has demonstrated exceptional performance on large-scale datasets such as SportsMOT [22] and DanceTrack [23], where varying motions and uniform appearances are present. Through the utilization of the same model, we have been able to attain comparable outcomes on MOT17 and MOT20.

II. RELATED WORK

Multi-object Tracking. Early research on multi-object tracking mainly relied on optimization algorithms [38]–[43] to solve the data association problem. However, with the advent of deep learning, tracking-by-detection using stronger detectors has become the dominant paradigm in multi-object tracking. In recent years, some approaches have fused detection and tracking tasks into a single network, benefiting from the success of multi-task learning [44] in neural networks. For instance, Tracktor [30] predicts an object’s position in the next frame by utilizing Faster RCNN’s [6] regression head, but it may fail at low frame rates. JDE [13] extends YOLOv3 [7] with a ReID branch to obtain object embedding for data association. To address the problem of detection and ReID tasks competing with each other in the JDE paradigm, Zhang *et al.* [14] designed FairMOT based on an anchor-free object detector, Centernet [8], achieving better tracking results. Additionally, ByteTrack [26] demonstrated that the performance bottleneck of trackers on mainstream multi-object tracking datasets, MOT [19], [20], is not in the association part but in the detection part. Thus, a powerful detector coupled with a simple hierarchical association strategy can achieve good tracking results.

Motion model. Motion estimation is crucial for object trackers, and in the early days, many classical multi-object tracking algorithms, such as SORT [24], DeepSORT [11], and MOTDT [25], use Kalman filters (KF) [31] to predict the inter-frame position offset of each object. However, the KF model is limited by its constant velocity assumption and performs poorly in complex situations and non-linear motion patterns.

To cope with these challenges, researchers have proposed various data-driven models. For example, Zhang *et al.* [27] used optical flow to obtain pixel-level motion information of objects, while CenterTrack [28] added an offset branch to an object detector to predict the motion information of the object center. Milan *et al.* [45] proposed an online tracker based on recurrent neural networks (RNNs) for multi-object tracking, and subsequent studies [46]–[48] applied RNNs to either fuse visual and motion information or calculate affinity scores for subsequent data association. ArtIST [29] and DEFT [32] used RNNs to predict the inter-frame motion of the target directly. TMOH [49] extended Tracktor [30] to use a simple linear model to predict the location of lost tracks, replacing visual cues for trajectory retracking.

Recent studies have also improved the KF to handle non-linear motion better. For example, MAT [50] proposed an IML module that considers both camera and pedestrian motion information, achieving better performance than the vanilla KF.

Cao *et al.* [51] recognized the limitations of the original KF in dealing with occlusion and non-linear motion and proposed corresponding improvements. They suggested that the KF should trust the recent observations more.

Despite these improvements, most of these studies are still based on the classical KF and its constant velocity model assumption. QuoVadis [52] improves the robustness of existing advanced trackers against long-term occlusions based on trajectory prediction in a bird’s eye view (BEV) scenario representation, consisting of several complex sub-modules that overcome the limitations of traditional methods.

Transformer-based methods. The recent success of transformer models in computer vision, particularly in the field of object detection, has led to the emergence of numerous transformer-based approaches. These include TransTrack [53], TrackFormer [21], TransCenter [54], and MOTR [55], which are contemporaneous online trackers based on DETR [56] and its variants. TrackFormer employs track queries to maintain object identities and utilizes heuristics to suppress duplicate tracks, as in Tracktor [30]. TransTrack directly employs previous object features as track queries to acquire tracking boxes and associates detection boxes based on IoU-matching. TransCenter obtains object center representation through transformer and performs tracking through CenterTrack’s object association [28]. Additionally, MOTR performs object tracking in an end-to-end manner by iteratively updating the track query, without requiring post-processing, making it a concise method. Furthermore, GTR [57] is an offline transformer-based tracker that employs queries to divide detected boxes into trajectories all at once, instead of generating tracking boxes. It should be noted that the training of all these models necessitates a high volume of training samples, expensive computational resources, and lengthy training times. In contrast, our methodology employs solely transformers for the purpose of extracting object motion information. Moreover, our proposed method necessitates only trajectory data as input and is characterized by its expeditious training process.

III. METHOD

The multi-object tracking task involves identifying the spatial and temporal locations of objects, i.e., their trajectories, in a given video sequence. The Transformer model, known for its ability to capture long-term dependencies, has proven highly effective in processing sequence data. Building on this success, we present a motion predictor that utilizes information about an object’s past temporal dynamics to predict its position in the next frame directly, as illustrated in Figure 2. Our data association approach relies solely on spatial similarity between the detection results of the current frame and the predicted position of the object. To accomplish this, we first propose a simple Transformer network in Section III-B to model the temporal dynamics of individual objects. Next, we introduce a Dynamic MLP, a MLP-like architecture that can explore channel-wise information. We further integrate it with the self-attention module to learn granularity information across token and channel levels in Section III-C. Finally, we study various augmentations to obtain complex motion patterns to improve

the understanding of motion dynamics. Overall, our approach leverages the strengths of the Transformer model and builds on it to develop an effective motion predictor for multi-object tracking.

A. Preliminary

The trajectory of an object consists of an ordered set of bounding boxes $\mathbf{T} = \{\mathbf{b}_{t_1}, \mathbf{b}_{t_2}, \dots\}$, where a bounding box is defined as $\mathbf{b}_t = \{x, y, w, h\}$, and t stands for the timestamp. At some moments, observations may be missing due to occlusion or detector failure, so the trajectory is not always continuous. \mathbf{D}_t is the set of detections of the t -th frame provided by an off-the-shelf detector.

Input representation. For each individual object, the motion predictor considers at most n_{past} of its past observations, \mathbf{X} , and predicts its position offsets, $\hat{\mathbf{O}}_t$, in the next frame. The past trajectory representation of the object can be denoted as a sequence $\mathbf{X} = (\dots, \mathbf{x}_{t-2}, \mathbf{x}_{t-1}) \in \mathbb{R}^{n \times 9}$. The object at moment $t - 1$ is denoted by \mathbf{x}_{t-1} , and its representation is defined as follows:

$$\mathbf{x}_{t-1} = (c_x, c_y, w, h, a, \delta_{c_x}, \delta_{c_y}, \delta_w, \delta_h), \quad (1)$$

where (c_x, c_y) represents the center coordinate of the object in the image plane, w, h and a stand for width, height and aspect ratio of its bounding box respectively. $\delta_{c_x}, \delta_{c_y}, \delta_w, \delta_h$ represent the change in their center position and width and height relative to the previous observation moment. Before being fed into the encoder layer for further processing, \mathbf{X} is embedded onto a higher dimensional space by a linear projection, i.e., $\bar{\mathbf{X}} = \mathbf{W}_x \mathbf{X} \in \mathbb{R}^{n \times d_m}$.

In order to make the input token sequence $\mathbf{E} \in \mathbb{R}^{n \times d_m}$ contain relative position information, we inject sinusoidal position encoding information to the input embeddings as in [35].

B. Vanilla Transformer-based Motion Predictor

The future motion of an object is significantly influenced by its past dynamic information. An intuitive approach utilises a vanilla Transformer encoder to capture the historical context of individual objects flexibly and efficiently. This encoder can extract a representation of the object’s trajectory history, where the primary component is the multi-head self-attention (MHSA) mechanism. By employing MHSA, the encoder can efficiently attend to various elements of the trajectory sequence and identify the most informative features that contribute to predicting the future motion of the object.

We compute the attention for every single object separately. The input sequence of tokens \mathbf{E} is linearly transformed to Q, K, V , which are the query, key, and value, respectively. For multi-head self-attention, a set of single-head attention jointly attends to information from different representation subspaces. The attention of a single head is calculated as by:

$$Attention(Q, K, V) = softmax\left(\frac{QK^T}{\sqrt{d_k}}\right)V, \quad (2)$$

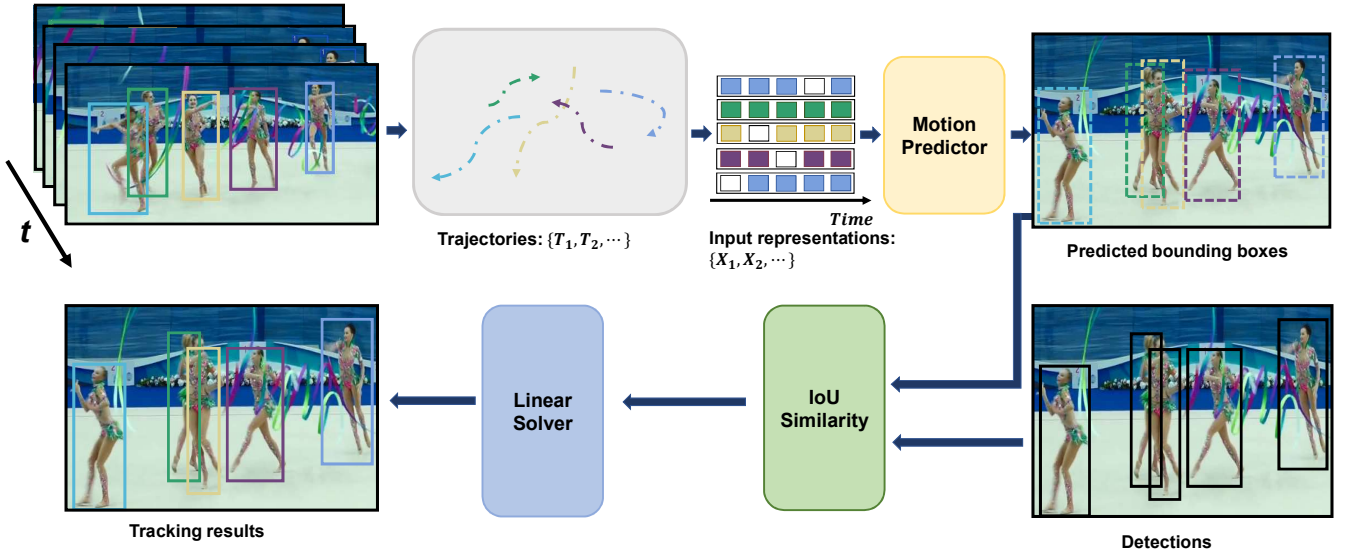


Fig. 2. An overview of the proposed method. The proposed motion predictor considers at most n_{past} of the historical observations of its trajectory when predicting the object position. With predicted bounding boxes, data association can be achieved by the linear solver, Hungarian algorithm, based solely on their spatial similarity to the current frame detection results. Blank boxes represent missing observations and dashed boxes represent predicted bounding boxes. Different colors represent different identities.

where d_k is the dimensionality of the corresponding hidden representation as a scaling factor. The multi-head attention variant with h heads, whose outputs are denoted as $head_0, head_1, \dots, head_i, \dots, head_h$,

$$head_i = Attention_i(Q_i, K_i, V_i), \quad (3)$$

where Q_i, K_i, V_i are the i_{th} part of Q, K and V . The outputs of h heads are cascaded and linearly transformed to obtain the final output.

Multi-object tracking is challenging because the interactions between objects, i.e., the effect of one object's behaviour on other objects, is a sophisticated process. Like some of the previous work [29], [58], [59], we also tried to model "interactions" between objects. We follow the Agentformer [60] and use an agent-aware attention mechanism to model multi-object motion in both temporal and social dimensions using sequential representations. We denote this method as *mult*.

C. Dual-granularity Information Fusion with Dynamic MLP

The utilization of token-level message passing across all channels lacks the capacity to adequately accommodate divergent semantics, thereby restricting their optimal exploitation and hence resulting in diminished efficacy [36], [37]. Therefore, there is a need to employ a more fine-grained message passing mechanism to cater to varying semantics in an adaptive manner. Such an approach can lead to more effective motion modeling by allowing for finer granularity in the communication of information between tokens. In this section, we emphasize the significance of implementing a more precise message-passing mechanism to facilitate adaptive treatment of diverse semantics in the context of motion modeling.

a) *Dynamic MLP*: Inspired by the above discovery, we explore a more powerful attention module named Dynamic MLP (DyMLP) to capture complicated motion patterns of objects further. It aggregates multiple positions distributed in different channels. As shown in Fig. 3, the core of DyMLP is the channel fusion layer (CFL), which consists of a dynamic fully-connected layer (DyFC) and an identity layer. Given the input token sequence $\mathbf{E} \in \mathbb{R}^{n \times d_m}$, for each token $e_i \in \mathbb{R}^{d_m}$, we first use a FC layer to predict d_m offsets: $\Delta = \{\delta_i\}_{i=1}^{d_m}$. Since there is no restriction on the generation of offsets, DyFC can aggregate temporal global channel information, as shown in Fig. 3. The basic DyFC operator can be formulated as below:

$$\begin{aligned} \hat{e}_i^T &= DyFC(e_i) = \tilde{e}_i \cdot \mathbf{W} + \mathbf{b}, \\ \tilde{e}_i &= [\mathbf{E}_{[i+\delta_1, 1]}, \mathbf{E}_{[i+\delta_2, 2]}, \dots, \mathbf{E}_{[i+\delta_{d_m}, d_m]}], \end{aligned} \quad (4)$$

where $\mathbf{W} \in \mathbb{R}^{d_m \times d_m}$ and $\mathbf{b} \in \mathbb{R}^{d_m}$ are learnable parameters. Besides, we preserve the original token information using identity layer and the output is \hat{e}_i^I . CFL outputs the fusion result as a weighted sum of \hat{e}_i^T and \hat{e}_i^I , which can be formulated as:

$$\hat{e} = \omega^T \odot \hat{e}^T + \omega^I \odot \hat{e}^I, \quad (5)$$

where \odot is the Hadamard product, $\omega^{\{T, I\}} \in \mathbb{R}^{d_m}$ are calculated from the following equation:

$$[\omega^I, \omega^T] = softmax([\mathbf{W}^I \cdot \hat{x}, \mathbf{W}^T \cdot \hat{x}]), \quad (6)$$

where $\hat{x} \in \mathbb{R}^{d_m}$ is the average summation of \hat{e}^T and \hat{e}^I , $\mathbf{W}^{\{I, T\}} \in \mathbb{R}^{d_m \times d_m}$ are learnable parameters and $softmax(\cdot)$ is the channel-wise normalization operation.

Hence, each encoder layer contains two sub-layers. We use residual connections [61] in both sub-layers and then

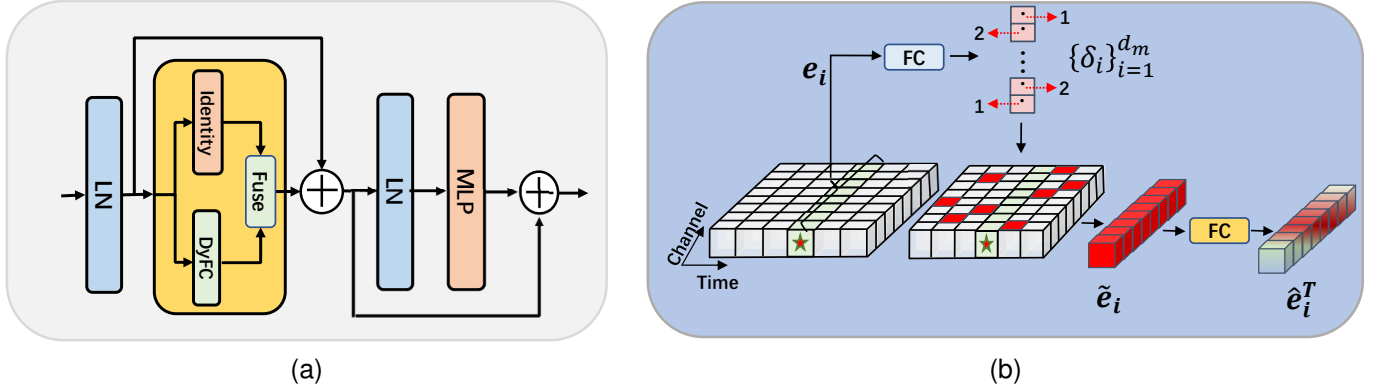


Fig. 3. The network structure of dynamic MLP is shown in (a), and the dynamic FC operation process is shown in (b).

perform layer normalization (LN) [62]. Mathematically, the whole process in the encoder layer can be described as follows:

$$\begin{aligned} \text{DIF}(E^{l-1}) &= \text{MHSA}(E^{l-1}) + \text{DyMLP}(E^{l-1}) \\ \hat{E}^l &= \text{LN}(\text{DIF}(E^{l-1})) + E^{l-1} \\ E^l &= \text{LN}(\text{FFN}(\hat{E}^l)) + \hat{E}^l, \end{aligned} \quad (7)$$

where l denotes the l -th layer and FFN for a feed forward network.

b) Dual-granularity Information Fusion Layer: With the proposed Dynamic MLP, we further fuse it with a self-attention module in Transformer [35], benefiting from information from both the token-level granularity and channel-level granularity. To this end, we present a Dual-granularity Information Fusion Layer (DualIF). As shown in Fig. 4, its backbone is composed of L encode layers connected sequentially. Specifically, each encode layer consists of two sub-modules: a parallel multi-head self-attention module and a dynamic MLP module. The former passes the token-level information of other tokens into the query based on the computed pairwise attention weights, while the latter adaptively performs feature fusion of context distributed at the channel level.

D. Training and inference

a) Data augmentation creates complex motion patterns: Like in other deep learning tasks, such as Centernet [8], Centertrack [28], and YOLOX [9], the incorporation of data augmentation is crucial in enhancing the performance of the model. The limited availability of motion cues within existing datasets, coupled with the variability of motion across diverse datasets, necessitates the exploration of novel augmentation strategies to augment the training samples and advance the proficiency of our predictor in modeling motion dynamics. In this study, we examine three distinct augmentation strategies aimed at enriching the training samples. These strategies correspond to various cases that must be handled by the motion model, namely object position jitter and motion mutations, detection noise, and newly initialized shorter trajectories.

- Random drop. In generating the target trajectory representation \mathbf{X} , we randomly ignore the observation \mathbf{b}

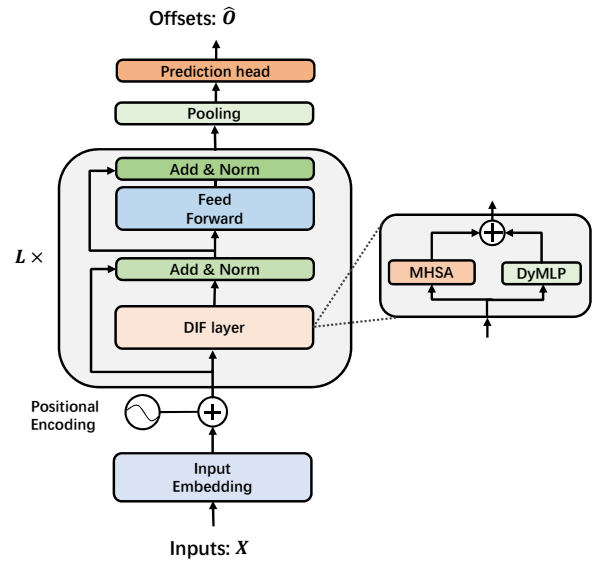


Fig. 4. The architecture of the proposed motion predictor.

with probability p_i . This strategy allows to simulate fast motion and low frame rate scenes.

- Spatial jitter. To enhance the robustness of the system against detection noise, it is a widely adopted practice to incorporate spatial jitter into the bounding boxes. This technique involves introducing small variations in the position and size of the bounding boxes during training. By doing so, the model becomes more resilient to variations in object localization due to detection noise. Furthermore, in a temporal sense, this approach also serves to augment the training dataset with a broader range of motion patterns.
- Random length. Due to the short new birth trajectory, there is little available temporal information. By randomly varying the length of the training sequence, the model is exposed to a diverse range of motion patterns, which enables it to learn to generalize to different temporal contexts. To mimic this, we train the motion model using a sequence of observations of arbitrary length (in range $[2, n_{past}]$) reserved for each object.

b) *Training loss*: We adopt the smooth loss L1 [63] to supervise the training process. Formally, given the predicted offsets, $\hat{\mathbf{O}} = \{\delta_{c_x}, \delta_{c_y}, \delta_w, \delta_h\}$, and corresponding ground truth \mathbf{O} , the loss is obtained by

$$L(\hat{\mathbf{O}}, \mathbf{O}) = \sum_{i \in \{c_x, c_y, w, h\}} \text{smooth}_{L_1}(\hat{\delta}_i - \delta_i), \quad (8)$$

in which

$$\text{smooth}_{L_1}(x) = \begin{cases} 0.5x^2 & \text{if } |x| < 1 \\ |x| - 0.5 & \text{otherwise.} \end{cases} \quad (9)$$

c) *Inference*: At first, we decode the predicted offset $\hat{\mathbf{O}}_t$ as the trajectory bounding boxes $\hat{\mathbf{D}}_t$ in the current frame. As with some classic online trackers [11], [24]–[26], we exploit a simple association algorithm. Detections are assigned to tracklets based on Intersection-over-Union(IoU) similarity between $\hat{\mathbf{D}}_t$ and \mathbf{D}_t using the Hungarian algorithm [64]. Unassigned detections are initialized as new trajectories. If no detection is assigned to a trajectory, the trajectory is marked as lost and if the time lost is greater than a given threshold, the target is considered out of view and removed from the trajectory set. Lost trajectories may also be retracked in the assignment step.

Given the detections from an object detector, our tracker associates identities over video sequences in an online manner, exploiting only motion cues. The overall tracking pipeline is shown in Algorithm 1. For brevity, trajectory rebirth is not shown.

Algorithm 1: Pseudo-code of MotionTrack.

Input: Detections: $D = \{\mathbf{b}_t^i | 1 \leq t \leq M, 1 \leq i \leq N_t\}$,
 Motion Predictor: MP, threshold for retaining a lost track t_{max} .
Output: Tracks T of the video

```

1 Initialization:  $T \leftarrow \emptyset$  and MP;
2 for  $t \leftarrow 1 : M$  do
3    $\mathbf{D}_t \leftarrow [\mathbf{b}_t^1, \dots, \mathbf{b}_t^{N_t}]$  // Detections of current
     frame.
4    $\hat{\mathbf{D}}_t \leftarrow [\hat{\mathbf{b}}_t^1, \dots, \hat{\mathbf{b}}_t^{|T|}]$  from  $T$  // Predicted
     bounding boxes
5    $\mathbf{C}_t \leftarrow C_{\text{IoU}}(\hat{\mathbf{D}}_t, \mathbf{D}_t)$  // Cost matrix based on
     IoU similarity
   /* Assign detections to tracks using
     Hungarian algorithm */
6    $\mathcal{M}, \mathcal{T}_u, \mathcal{D}_u \leftarrow \text{assignment}(\mathbf{C}_t)$ 
7    $T \leftarrow \{T_i(\mathbf{b}_t^j), \forall (i, j) \in \mathcal{M}\}$  // Update the
     matched tracks
8    $T \leftarrow \{T_i.age + 1, \forall (i) \in \mathcal{T}_u\}$ 
9    $T \leftarrow \{T_i(D_j), \forall j \in \mathcal{D}_u, i = |T| + 1\}$ 
10  Kill lost tracks with age  $\geq t_{max}$ 
11  for  $T$  in  $T$  do
12    | MP( $T$ ) // Predict motion of tracks
13  end
14 end
```

datasets, namely MOT17 [19], MOT20 [20], SportsMOT [22] and DanceTrack [23]. MOT17 is a commonly used benchmark in the field of multi-pedestrian tracking and comprises video sequences captured from moving and still cameras, from different viewpoints and with varying frame rates. It consists of seven training sequences and seven test sequences. MOT20, on the other hand, is also a pedestrian tracking dataset, but with more crowded recorded scenes as compared to MOT17. The SportsMOT dataset offers video clips of three different sports categories, i.e., basketball, football, and volleyball. These clips are collected from various sources such as the Olympic Games, NCAA Championship, and NBA on YouTube, and cover a wide range of complex sports scenes captured from different perspectives. The dataset contains 45 video clips in both the training and validation sets. Due to the similar appearance of athletes and the complex motion scenarios, SportsMOT requires a high level of robustness in tracking algorithms. Dancetrack, on the other hand, is a recently proposed dataset that offers more training and evaluation videos. Objects in this dataset possess highly similar appearance, are severely occluded from each other, and exhibit nonlinear motion at a high degree, making it challenging for existing advanced approaches based on appearance and motion information. Therefore, we aim to propose a better motion model that can improve the tracking algorithm’s ability to cope with frequent crossings and nonlinear motions. SportsMOT and Dancetrack datasets provide ideal benchmarks for evaluating the performance of tracking algorithms.

Evaluation Metrics. To evaluate our algorithm, we adapt the Higher Order Metric (HOTA, AssA, DetA) [65], IDF1 [66] and the CLEAR metrics (MOTA, FP, FN, IDs, *et al.*) [67] to assess different aspects of the tracking algorithm. MOTA is calculated from FN, FP, IDs and is susceptible to the influence of detection results. IDF1 focuses on measuring association performance. HOTA is designed to fairly combine evaluation of detection and association, and therefore, we use it as the primary metric.

B. Implementation Details

Our primary focus is on developing a motion model for tracking objects. For this purpose, we use the publicly available YOLOX detector weights provided by ByteTrack [26] and DanceTrack [23] separately to detect objects in the MOT and DanceTrack datasets. The motion predictor includes $L = 6$ encode layers, and the input token dimension d_m is set to 512. The multi-head self-attention uses 8 heads, and the drop probability for data augmentation during training is set to $p_i = 0.1$. We set the maximum historical observation window value n_{past} to 10, and the batch size to 64. We use the Adam optimizer [68] with $\beta_1 = 0.9$, $\beta_2 = 0.98$ and $\epsilon = 10^{-8}$. The learning rate is adjusted dynamically during training following the approach proposed in [35].

IV. EXPERIMENTS

A. Datasets and Metrics

Datasets. In order to conduct a comprehensive evaluation of the proposed algorithm, we performed experiments on four

C. Benchmark Evaluation

We assessed the efficacy of the proposed method by testing it on four datasets comprising various motion patterns. The

TABLE I

COMPARISON TO THE SORT-LIKE TRACKERS ON SPORTSMOT VALIDATION SET. THE BEST RESULTS ARE SHOWN IN **BOLD**. \uparrow : HIGHER BETTER.

Tracker	HOTA \uparrow	DetA \uparrow	AssA \uparrow	MOTA \uparrow	IDF1 \uparrow
SORT [24]	64.9	80.0	62.8	93.3	69.9
ByteTrack [26]	64.4	76.8	64.1	93.4	73.7
OC_SORT [51]	71.2	85.9	59.1	93.4	72.4
Ours	72.8	84.7	62.6	92.0	74.9

TABLE II

COMPARISON TO THE STATE-OF-THE-ARTS ON DANCETRACK TEST SET. THE BEST RESULTS ARE SHOWN IN **BOLD**. \uparrow : HIGHER BETTER. * INDICATES THAT THE MOTION MODEL IS TRAINED ON DANCETRACK TRAINING SET.

Tracker	HOTA \uparrow	DetA \uparrow	AssA \uparrow	MOTA \uparrow	IDF1 \uparrow
CenterTrack [28]	41.8	78.1	22.6	86.8	35.7
FairMOT [14]	39.7	66.7	23.8	82.2	40.8
QDTrack [69]	45.7	72.1	29.2	83.0	44.8
TransTrk [53]	45.5	75.9	27.5	88.4	45.2
TraDes [70]	43.3	74.5	25.4	86.2	41.2
SORT [24]	47.9	72.0	31.2	91.8	50.8
DeepSORT [11]	45.6	71.0	29.7	87.8	47.9
ByteTrack [26]	47.3	71.6	31.4	89.5	52.5
MOTR [55]	54.2	73.5	40.2	79.7	51.5
OC_SORT [51]	55.1	80.3	38.0	89.4	54.2
Ours*	52.9	80.9	34.7	91.3	53.8
Ours	58.2	81.4	41.7	91.3	58.6

models marked with an asterisk (*) were trained on the corresponding dataset’s training set, whereas those without an asterisk were trained on the SportsMOT training set. We investigate the effect of different training sets on the model performance in Tab. V.

SportsMOT. Since SportsMOT’s test dataset evaluation platform has closed, we use its validation set as a test set to evaluate the SORT-like approaches. For a fair comparison, all methods use the same YOLOX detector trained on the SportsMOT training set. The results of the evaluation, as presented in Table I, demonstrate that our proposed approach has a significant advantage over the classical Kalman filter-based SORT and ByteTrack approaches, as measured by the HOTA and IDF1 metrics, which evaluate the tracker’s ability to associate object instances. Specifically, our proposed approach outperforms SORT [24] by up to 7.9% in HOTA and 5.0% in IDF1. Additionally, our approach surpasses OC_SORT, indicating the superior performance of our proposed tracker in scenarios featuring complex motion.

DanceTrack. Table II presents a comparison between our proposed method and the current state-of-the-art techniques on the Dancetrack test set. It should be emphasized that the outcomes reported for our method were submitted to the Dancetrack test server without any post-processing, and the results indicate that our approach outperforms the other methods. Specifically, our method achieves a higher HOTA score, which is 3.1 percentage points better than the OC_SORT [51] method that enhances the Kalman filter. Furthermore, in the evaluation metrics that concentrate on measuring tracking performance, namely AssA and IDF1, our approach leads by 3.7% and 4.4%, respectively. These findings suggest that our proposed data-driven motion model outperforms SORT-like

TABLE III

RESULTS ON MOT17 TEST DATASET UNDER THE PRIVATE DETECTION PROTOCOLS. THE BEST RESULTS ARE SHOWN IN **BOLD**. \uparrow : HIGHER BETTER AND \downarrow : LOWER BETTER. * INDICATES THAT THE MOTION MODEL IS TRAINED ON MOT17 TRAINING SET.

Tracker	HOTA \uparrow	MOTA \uparrow	IDF1 \uparrow	AssA \uparrow	AssR \uparrow
FairMOT [14]	59.3	73.7	72.3	58.0	63.6
TransCt [54]	54.5	73.2	62.2	49.7	54.2
TransTrk [53]	54.1	75.2	63.5	47.9	57.1
CSTrack [71]	59.3	74.9	72.6	57.9	63.2
QDTrack [69]	53.9	68.7	66.3	52.7	57.2
PermaTr [72]	55.5	73.8	68.9	53.1	59.8
MOTR [55]	57.2	71.9	68.4	55.8	59.2
ByteTrack [26]	63.1	80.3	77.3	62.0	68.2
OC_SORT [51]	63.2	78.0	77.5	63.2	67.5
Ours*	60.9	76.5	73.5	59.4	66.0
Ours	61.6	78.6	75.1	60.2	66.7

TABLE IV

RESULTS ON MOT20 TEST DATASET UNDER THE PRIVATE DETECTION PROTOCOLS. THE BEST RESULTS ARE SHOWN IN **BOLD**. \uparrow : HIGHER BETTER AND \downarrow : LOWER BETTER. * INDICATES THAT THE MOTION MODEL IS TRAINED ON MOT20 TRAINING SET.

Tracker	HOTA \uparrow	MOTA \uparrow	IDF1 \uparrow	AssA \uparrow	AssR \uparrow
FairMOT [14]	54.6	61.8	67.3	54.7	60.7
TransCt [54]	43.5	58.5	49.6	37.0	45.1
CSTrack [71]	54.0	66.6	68.6	54.0	57.6
ByteTrack [26]	61.3	77.8	75.2	59.6	66.2
QuoVadis [52]	61.5	80.3	75.7	59.9	67.0
OC_SORT [51]	62.1	75.5	75.9	62.0	67.5
Ours*	58.3	75.0	53.9	52.3	63.5
Ours	59.7	76.4	71.3	56.8	63.5

techniques [11], [24], [26] based on the standard Kalman filter [31]. Additionally, our method surpasses the advanced fully end-to-end MOTR [55] method. These results provide evidence that our proposed motion model can effectively model the temporal motion of objects and achieve superior performance in dealing with complex motion scenes.

MOT17 & MOT20. We further directly conduct experiments on the MOT17 test set with the model that obtained state-of-the-art performance on Dancetrack to verify the generality of the proposed motion model. As can be seen in Tab. III and Tab. IV, without any tailored tuning, our approach still achieves comparable performance with advanced methods. Since the MOT17 and MOT20 contains video sequences taken at different resolutions and under different lighting conditions, detection becomes a key factor affecting tracking performance. Just like MOTR, we also believe that MOT benchmarks has limitations and cannot fully measure the tracking performance of our method. It is only used to verify that the proposed method has good generality.

D. Ablation Study

We conduct ablation studies on the validation set of DanceTrack [23] to investigate the impact of different training data, model components, data augmentation methods, and some hyper-parameters on the proposed method.

Impact of training datasets. In this subsection, we compare the effect of different training data on the model performance. As shown in Tab. V, The best performance is obtained with

TABLE V
ABLATION ON DIFFERENT TRAINING SETS.

Training dataset	HOTA↑	DetA↑	AssA↑	MOTA↑	IDF1↑
DanceTrack	51.8	78.0	34.6	89.3	52.0
MOT17+SportsMOT	53.2	78.4	36.3	89.2	53.5
Dance+SportsMOT	52.7	78.6	35.5	89.2	52.7
SportsMOT	54.6	78.6	38.1	89.2	54.6

TABLE VI
ABLATION ON DIFFERENT DATA AUGMENTATION STRATEGIES. 'D' STANDS FOR RANDOM DROP, 'J' STANDS FOR RANDOM JITTER AND 'L' STANDS FOR RANDOM LENGTH.

NUM		HOTA↑	DetA↑	AssA↑	MOTA↑	IDF1↑
①	No aug.	53.5	78.6	36.5	89.3	53.5
	+ D	54.3	78.4	37.8	89.2	54.2
	+ J	54.4	78.6	37.8	89.2	54.5
	+ D + J	54.6	78.6	38.1	89.2	54.6
	+ D + J + L	53.5	78.7	36.5	89.3	53.5
②	+ L	52.4	78.6	35.1	89.2	52.6
	+ D + L	53.9	78.5	37.1	89.3	53.9
	+ J + L	54.1	78.2	37.6	89.3	54.5

models trained only on SportsMOT training set. Our hypothesis to support this observation is that SportsMOT comprises a more diverse range of motion patterns, characterized by faster and more irregular athlete movements. Conversely, pedestrian movements in MOT17 are generally linear, while Dancetrack captures static scenes with a limited scope of movement.

Impact of different data augmentations. As delineated in Section III-C, we introduce a triad of data augmentation strategies, namely Random drop, Spatial jitter, and Random length. To investigate the efficacy of these methods, we conducted a comparative analysis using the performance metric HOTA. The results of this experiment are illustrated in Table VI (①). It is worth noting that using Random drop and Spatial jitter brings a HOTA improvement of 0.8 and 0.9 percentage points, respectively, compared to not using any data augmentation. Using both technologies at the same time brought a 1.1 percentage point improvement. However, when Random length is added to the augmentation process, a decrease in performance is observed. To verify this trend, we conducted a second set of experiments as detailed in Table VI (②), which confirmed that Random length did not contribute to any positive benefit. Based on these results, we decide to retain only the first two data augmentation techniques, namely Random drop and Spatial jitter.

Impact of motion modelling. To validate the efficacy of the proposed motion predictor, we conducted a comparative analysis with several existing motion models. As illustrated in Table VII, the outcomes demonstrate that incorporating motion information yields significantly better performance than those not using motion information (i.e. only naive IoU association). Furthermore, the HOTA metrics reveal that our approach outperforms Kalman filter [31], which relies on linear motion hypothesis, by 8.2%, and LSTM [32], which employs a recurrent neural network, by 3.4%, respectively. This notable improvement in performance is attributed to the dual-granularity information incorporated in our motion model, which provides a global temporal perspective and

TABLE VII
COMPARING DIFFERENT MOTION MODELS.

	HOTA↑	DetA↑	AssA↑	MOTA↑	IDF1↑
No motion	44.7	79.6	25.3	87.3	36.8
Kalman filter	46.8	70.2	31.3	87.5	52.1
LSTM	51.2	76.7	34.3	87.1	51.6
Ours	54.6	78.6	38.1	89.2	54.6

TABLE VIII
ABLATION STUDY ON DIFFERENT COMPONENTS. "MHSA" STANDS FOR MULTI-HEAD SELF-ATTENTION, "DyMLP" FOR DYNAMIC MLP.

	HOTA↑	DetA↑	AssA↑	MOTA↑	IDF1↑
w/o MHSA	53.6	78.0	37.0	89.2	54.1
w/o DyMLP	53.0	78.6	35.8	89.1	53.2
Ours	54.6	78.6	38.1	89.2	54.6

TABLE IX
EVALUATION OF THE IMPACT OF INTER-OBJECT INTERACTIONS. *Mult.* DENOTES THE METHOD OF MODELING INTER-TARGET INTERACTIONS USING AGENT-AWARE ATTENTION.

	HOTA↑	DetA↑	AssA↑	MOTA↑	IDF1↑
<i>Mult.</i>	53.1	78.9	35.9	89.2	53.0
Ours	54.6	78.6	38.1	89.2	54.6

thereby improves motion learning.

Impact of model components. To further investigate the impact of the key components of our motion predictor, we conducted an ablation study by removing them individually and evaluating the resulting model’s performance. The results of this study are presented in Table VIII. As shown in the table, when the MHSA module and the DyMLP module are removed separately from the motion predictor, there is a decline in the HOTA metric by 1% and 1.6%, respectively. Moreover, the association score (AssA) also suffers a reduction of 1.1% and 2.3%, respectively. These findings highlight the crucial role of both token-level and channel-level feature fusion in learning motion models that capture the object’s temporal dynamics effectively.

Does the interaction between objects help? In the context of multi-object tracking, it is pertinent to consider object interactions due to the complexity of the task. In this part, we adopt the Encoder component of AgentFormer [60] to implement an object-aware attention mechanism that jointly models the temporal and social dimensions of multi-object trajectories using a sequence representation. It is noteworthy that conventional trajectory prediction tasks typically require a complete history of the target’s past trajectory to predict a fixed-length future trajectory. To adapt this, *mult* (see Sec. III-B) utilizes a sequence representation of multi-object trajectories by concatenating trajectory features across time and objects. Unlike traditional trajectory prediction tasks, the number of targets in multi-object tracking varies over time and the target trajectories may not be continuous at all time. To adapt the agent-aware attention mechanism, we employ learnable embeddings to fill in the missing objects’ representation within the maximum observation window of n_{past} . Consequently, the *mult* can be considered as a trajectory prediction task that is consistent with AgentFormer but predicts only a single time



Fig. 5. Qualitative comparison between MotionTrack and OC_SORT [51] on DanceTrack validation. Each pair of rows shows the results comparison for one sequence. The color of the bounding boxes represents the identity of the tracks. To be exactly, the ID switch in (a) occurs between frame #45 → #54; (c) #310 → #333; (e) #432 → #441.

TABLE X
IMPACT OF RANDOM DROP PROBABILITY p_i DURING TRAINING.

p_i	HOTA↑	DetA↑	AssA↑	MOTA↑	IDF1↑
0	53.5	78.6	36.5	89.3	53.5
0.1	54.3	78.4	37.8	89.2	54.2
0.2	54.0	78.6	37.3	89.2	54.1
0.3	53.6	78.7	36.6	89.3	54.2

step. Our experimental results, as presented in Tab. IX, reveal that in scenarios with multiple motion patterns created by choreographers, modeling of inter-target interaction does not enhance the performance of multi-object tracking. We must emphasize that our study only explores the potential of joint attention-based social and temporal modeling. Other methods may be effective.

Impact of random drop probability during training. The

approach of randomly dropping a historical observation with a certain probability p_i enables the generation of more complex motion patterns, such as rapid movements of an object. The impact of different values of p_i on the tracking performance is investigated in Table X. The results indicate that as p_i gradually increases from 0 to 0.3, the performance of the tracking method varies. Notably, the highest score on the HOTA metric is achieved when p_i is set to 0.1. This finding suggests that a moderate level of dropping historical observations can enhance the tracking performance, while excessively high probabilities of dropping such observations may have a negative impact on the tracking quality.

Impact of different memory pooling types. The motion predictor proposed in this study utilizes the encoder of a Transformer to capture the temporal dynamics of an object, resulting in the generation of memory. To feed this memory to



Fig. 6. **Illustration of failure cases.** We show the two most common failure cases of our approach. In the first row, due to the rapid movement of the on-board camera during the corner and the occlusion, we can observe an ID switch (257 and 290) of the man in the black suit. In the second row, we can see the identity switch (79 and 113) occur when the lady in the grey T-shirt, leaving the camera, reappears.

TABLE XI
COMPARISON OF DIFFERENT POOLING TYPES.

	HOTA \uparrow	DetA \uparrow	AssA \uparrow	MOTA \uparrow	IDF1 \uparrow
<i>sum</i>	51.7	78.2	34.3	89.2	51.9
<i>last</i>	53.8	78.7	37.0	89.2	54.0
<i>mean</i>	54.6	78.6	38.1	89.2	54.6

TABLE XII
THE IMPACT OF MAXIMUM HISTORICAL OBSERVATION WINDOW.

n_{past}	HOTA \uparrow	DetA \uparrow	AssA \uparrow	MOTA \uparrow	IDF1 \uparrow
3	51.6	78.2	34.2	89.2	51.2
5	52.3	78.2	35.2	89.2	52.8
10	54.6	78.6	38.1	89.2	54.6
13	54.2	78.3	37.8	89.1	54.1
15	53.3	78.4	36.4	89.1	53.3

the regression head, a pooling operation is necessary. Specifically, we explore three different types of pooling operations, namely *mean*, *sum*, and *last*, which respectively refer to taking the mean value of the encoder memory along the time dimension, summing the memory, or utilizing the last moment representation. The results presented in Table XI demonstrate that the *mean* pooling operation achieves the best performance among the three tested options.

Impact of maximum historical observation window. As presented in Tab. XII, very small historical observation windows fail to provide sufficient information, resulting in inaccurate predictions. In contrast, very large historical observation windows introduce a considerable amount of noise, leading to degraded performance. Based on the results, we set the value of n_{past} to 10, as it attains the best performance across all metrics. This finding highlights the importance of selecting an appropriate value for the historical observation window size to achieve optimal performance in object tracking tasks.

Qualitative Results. To get a more intuitive picture of MotionTrack’s superiority over OC_SORT, we provide more visualization for the comparison. In Figure 5, we show additional samples where OC_SORT suffers from ID switch caused by non-linear motion or occlusion but our method successfully copes. In addition, We show some qualitative results of our method on SportsMOT in Fig. 7.

V. LIMITATIONS

While our approach acquires simplicity and generality by relying solely on motion modeling, we have also identified

certain challenges associated with this paradigm. We observe that our model struggles to handle video sequences taken from the first view, especially when superimposing fast camera movements and long-term object loss. We present two typical examples of failure in Fig. 6.

VI. CONCLUSION

In this paper, we propose a novel online tracker that utilizes a learnable motion predictor. The proposed approach incorporates two distinct modules to capture information at varying levels of granularity, thus enabling efficient modeling of an object’s temporal dynamics. Specifically, we employ Transformer networks for motion prediction, which are capable of capturing complex motion patterns at the token level. We further introduce DyMLP, a MLP-like architecture, to extract semantic information distributed across different channels. By integrating DyMLP with the self-attention module in Transformer, our approach leverages the dual-granularity information to achieve superior performance. The results of our experiments have illustrated that the proposed methodology surpasses current state-of-the-art techniques when applied to datasets that feature intricate motion scenarios. Additionally, the performance of the proposed method has exhibited its resilience in the face of complex motion patterns.

REFERENCES

- [1] L. Wen, D. Du, Z. Cai, Z. Lei, M.-C. Chang, H. Qi, J. Lim, M.-H. Yang, and S. Lyu, “Ua-detrac: A new benchmark and protocol for multi-object detection and tracking,” *Computer Vision and Image Understanding*, vol. 193, p. 102907, 2020.

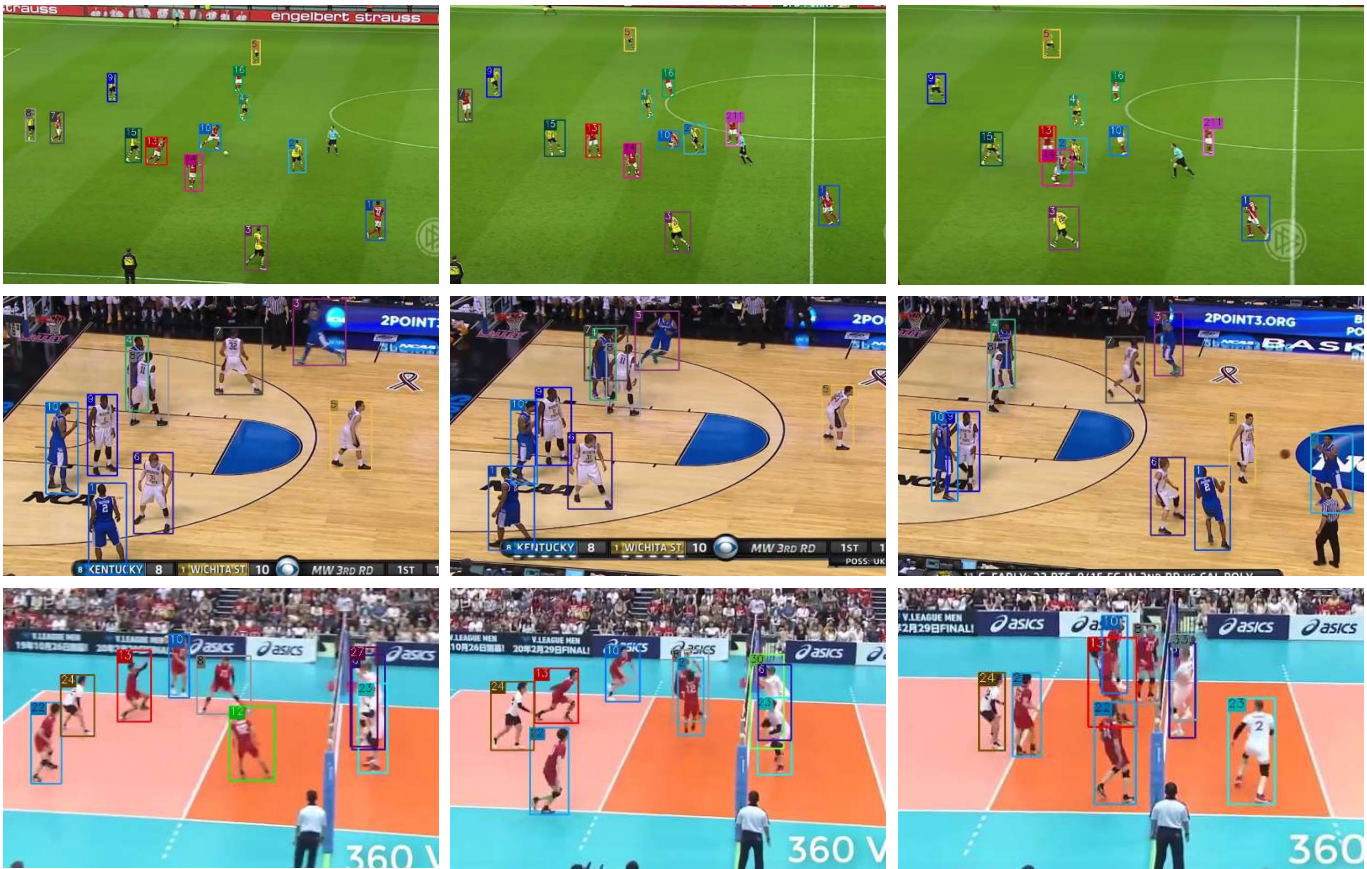


Fig. 7. Qualitative results of our method on SportsMOT. Different colored bounding boxes indicate different identity. Best viewed in color and zoom in.

[2] Y. Yuan, U. Iqbal, P. Molchanov, K. Kitani, and J. Kautz, “Glamr: Global occlusion-aware human mesh recovery with dynamic cameras,” in *Proceedings of the IEEE/CVF Conference on Computer Vision and Pattern Recognition*, 2022, pp. 11 038–11 049.

[3] H. Caesar, V. Bankiti, A. H. Lang, S. Vora, V. E. Liong, Q. Xu, A. Krishnan, Y. Pan, G. Baldan, and O. Beijbom, “nusenes: A multimodal dataset for autonomous driving,” in *Proceedings of the IEEE/CVF conference on computer vision and pattern recognition*, 2020, pp. 11 621–11 631.

[4] P. Sun, H. Kretzschmar, X. Dotiwalla, A. Chouard, V. Patnaik, P. Tsui, J. Guo, Y. Zhou, Y. Chai, B. Caine *et al.*, “Scalability in perception for autonomous driving: Waymo open dataset,” in *Proceedings of the IEEE/CVF conference on computer vision and pattern recognition*, 2020, pp. 2446–2454.

[5] R. Martin-Martin, M. Patel, H. Rezatofighi, A. Sheno, J. Gwak, E. Frankel, A. Sadeghian, and S. Savarese, “Jrdb: A dataset and benchmark of egocentric robot visual perception of humans in built environments,” *IEEE transactions on pattern analysis and machine intelligence*, 2021.

[6] S. Ren, K. He, R. Girshick, and J. Sun, “Faster r-cnn: Towards real-time object detection with region proposal networks,” *Advances in neural information processing systems*, vol. 28, 2015.

[7] J. Redmon and A. Farhadi, “Yolov3: An incremental improvement,” *arXiv preprint arXiv:1804.02767*, 2018.

[8] X. Zhou, D. Wang, and P. Krähnenbühl, “Objects as points,” in *arXiv preprint arXiv:1904.07850*, 2019.

[9] Z. Ge, S. Liu, F. Wang, Z. Li, and J. Sun, “Yolox: Exceeding yolo series in 2021,” *arXiv preprint arXiv:2107.08430*, 2021.

[10] K. Yang, D. Li, and Y. Dou, “Towards precise end-to-end weakly supervised object detection network,” in *Proceedings of the IEEE/CVF International Conference on Computer Vision*, 2019, pp. 8372–8381.

[11] N. Wojke, A. Bewley, and D. Paulus, “Simple online and realtime tracking with a deep association metric,” in *2017 IEEE international conference on image processing (ICIP)*. IEEE, 2017, pp. 3645–3649.

[12] A. Hermans, L. Beyer, and B. Leibe, “In defense of the triplet loss for person re-identification,” *arXiv preprint arXiv:1703.07737*, 2017.

[13] Z. Wang, L. Zheng, Y. Liu, Y. Li, and S. Wang, “Towards real-time multi-object tracking,” in *European Conference on Computer Vision*. Springer, 2020, pp. 107–122.

[14] Y. Zhang, C. Wang, X. Wang, W. Zeng, and W. Liu, “Fairmot: On the fairness of detection and re-identification in multiple object tracking,” *International Journal of Computer Vision*, vol. 129, pp. 3069–3087, 2021.

[15] A. A. Mekonnen and F. Lerasle, “Comparative evaluations of selected tracking-by-detection approaches,” *IEEE Transactions on Circuits and Systems for Video Technology*, vol. 29, no. 4, pp. 996–1010, 2018.

[16] X. Chen, Z. Qin, L. An, and B. Bhanu, “Multiperson tracking by online learned grouping model with nonlinear motion context,” *IEEE Transactions on Circuits and Systems for Video Technology*, vol. 26, no. 12, pp. 2226–2239, 2015.

[17] J. Kong, E. Mo, M. Jiang, and T. Liu, “Motfr: Multiple object tracking based on feature recoding,” *IEEE Transactions on Circuits and Systems for Video Technology*, vol. 32, no. 11, pp. 7746–7757, 2022.

[18] F. Wang, L. Luo, and E. Zhu, “Two-stage real-time multi-object tracking with candidate selection,” in *International Conference on Multimedia Modeling*. Springer, 2021, pp. 49–61.

[19] A. Milan, L. Leal-Taixé, I. Reid, S. Roth, and K. Schindler, “Mot16: A benchmark for multi-object tracking,” *arXiv preprint arXiv:1603.00831*, 2016.

[20] P. Dendorfer, H. Rezatofighi, A. Milan, J. Shi, D. Cremers, I. Reid, S. Roth, K. Schindler, and L. Leal-Taixé, “Mot20: A benchmark for multi object tracking in crowded scenes,” *arXiv preprint arXiv:2003.09003*, 2020.

[21] T. Meinhardt, A. Kirillov, L. Leal-Taixe, and C. Feichtenhofer, “Trackformer: Multi-object tracking with transformers,” in *The IEEE Conference on Computer Vision and Pattern Recognition (CVPR)*, June 2022.

[22] Y. Li, L. Chen, R. He, Z. Wang, G. Wu, and L. Wang, “Multisports: A multi-person video dataset of spatio-temporally localized sports actions,”

- in *Proceedings of the IEEE/CVF International Conference on Computer Vision*, 2021, pp. 13 536–13 545.
- [23] P. Sun, J. Cao, Y. Jiang, Z. Yuan, S. Bai, K. Kitani, and P. Luo, “Dancetrack: Multi-object tracking in uniform appearance and diverse motion,” in *Proceedings of the IEEE/CVF Conference on Computer Vision and Pattern Recognition*, 2022, pp. 20993–21 002.
- [24] A. Bewley, Z. Ge, L. Ott, F. Ramos, and B. Upcroft, “Simple online and realtime tracking,” in *2016 IEEE international conference on image processing (ICIP)*. IEEE, 2016, pp. 3464–3468.
- [25] C. Long, A. Haizhou, Z. Zijie, and S. Chong, “Real-time multiple people tracking with deeply learned candidate selection and person re-identification,” in *ICME*, 2018.
- [26] Y. Zhang, P. Sun, Y. Jiang, D. Yu, F. Weng, Z. Yuan, P. Luo, W. Liu, and X. Wang, “Bytetrack: Multi-object tracking by associating every detection box,” in *European Conference on Computer Vision*. Springer, 2022, pp. 1–21.
- [27] J. Zhang, S. Zhou, X. Chang, F. Wan, J. Wang, Y. Wu, and D. Huang, “Multiple object tracking by flowing and fusing,” in *The IEEE Conference on Computer Vision and Pattern Recognition (CVPR)*, 2020.
- [28] X. Zhou, V. Koltun, and P. Krähenbühl, “Tracking objects as points,” in *European Conference on Computer Vision*. Springer, 2020, pp. 474–490.
- [29] F. Saleh, S. Aliakbarian, H. Rezaatofighi, M. Salzmann, and S. Gould, “Probabilistic tracklet scoring and inpainting for multiple object tracking,” in *Proceedings of the IEEE/CVF Conference on Computer Vision and Pattern Recognition*, 2021, pp. 14 329–14 339.
- [30] P. Bergmann, T. Meinhardt, and L. Leal-Taixé, “Tracking without bells and whistles,” in *Proceedings of the IEEE/CVF International Conference on Computer Vision*, 2019, pp. 941–951.
- [31] R. E. Kalman *et al.*, “Contributions to the theory of optimal control,” *Bol. soc. mat. mexicana*, vol. 5, no. 2, pp. 102–119, 1960.
- [32] M. Chaabane, P. Zhang, R. Beveridge, and S. O’Hara, “Deft: Detection embeddings for tracking,” *arXiv preprint arXiv:2102.02267*, 2021.
- [33] W. Luo, B. Yang, and R. Urtasun, “Fast and furious: Real time end-to-end 3d detection, tracking and motion forecasting with a single convolutional net,” in *Proceedings of the IEEE conference on Computer Vision and Pattern Recognition*, 2018, pp. 3569–3577.
- [34] S. Bai, J. Z. Kolter, and V. Koltun, “An empirical evaluation of generic convolutional and recurrent networks for sequence modeling,” *arXiv preprint arXiv:1803.01271*, 2018.
- [35] A. Vaswani, N. Shazeer, N. Parmar, J. Uszkoreit, L. Jones, A. N. Gomez, Ł. Kaiser, and I. Polosukhin, “Attention is all you need,” *Advances in neural information processing systems*, vol. 30, 2017.
- [36] D. Bau, J.-Y. Zhu, H. Strobelt, A. Lapedriza, B. Zhou, and A. Torralba, “Understanding the role of individual units in a deep neural network,” *Proceedings of the National Academy of Sciences*, vol. 117, no. 48, pp. 30 071–30 078, 2020.
- [37] Z. Wu, D. Lischinski, and E. Shechtman, “StyleSpace analysis: Disentangled controls for stylegan image generation,” in *Proceedings of the IEEE/CVF Conference on Computer Vision and Pattern Recognition*, 2021, pp. 12 863–12 872.
- [38] A. Roshan Zamir, A. Dehghan, and M. Shah, “Gmcp-tracker: Global multi-object tracking using generalized minimum clique graphs,” in *European conference on computer vision*. Springer, 2012, pp. 343–356.
- [39] L. Wen, W. Li, J. Yan, Z. Lei, D. Yi, and S. Z. Li, “Multiple target tracking based on undirected hierarchical relation hypergraph,” in *Proceedings of the IEEE conference on computer vision and pattern recognition*, 2014, pp. 1282–1289.
- [40] L. Lan, D. Tao, C. Gong, N. Guan, and Z. Luo, “Online multi-object tracking by quadratic pseudo-boolean optimization,” in *IJCAI*, 2016, pp. 3396–3402.
- [41] H. Sheng, Y. Zhang, J. Chen, Z. Xiong, and J. Zhang, “Heterogeneous association graph fusion for target association in multiple object tracking,” *IEEE Transactions on Circuits and Systems for Video Technology*, vol. 29, no. 11, pp. 3269–3280, 2018.
- [42] H. Sheng, J. Chen, Y. Zhang, W. Ke, Z. Xiong, and J. Yu, “Iterative multiple hypothesis tracking with tracklet-level association,” *IEEE Transactions on Circuits and Systems for Video Technology*, vol. 29, no. 12, pp. 3660–3672, 2018.
- [43] W. Feng, L. Lan, Y. Luo, Y. Yu, X. Zhang, and Z. Luo, “Near-online multi-pedestrian tracking via combining multiple consistent appearance cues,” *IEEE Transactions on Circuits and Systems for Video Technology*, vol. 31, no. 4, pp. 1540–1554, 2020.
- [44] Y. Zhang and Q. Yang, “A survey on multi-task learning,” *IEEE Transactions on Knowledge and Data Engineering*, 2021.
- [45] A. Milan, S. H. Rezaatofighi, A. Dick, I. Reid, and K. Schindler, “Online multi-target tracking using recurrent neural networks,” in *Thirty-First AAAI conference on artificial intelligence*, 2017.
- [46] X. Wan, J. Wang, and S. Zhou, “An online and flexible multi-object tracking framework using long short-term memory,” in *Proceedings of the IEEE Conference on Computer Vision and Pattern Recognition Workshops*, 2018, pp. 1230–1238.
- [47] A. Sadeghian, A. Alahi, and S. Savarese, “Tracking the untrackable: Learning to track multiple cues with long-term dependencies,” in *Proceedings of the IEEE international conference on computer vision*, 2017, pp. 300–311.
- [48] N. Ran, L. Kong, Y. Wang, and Q. Liu, “A robust multi-athlete tracking algorithm by exploiting discriminant features and long-term dependencies,” in *International Conference on Multimedia Modeling*. Springer, 2019, pp. 411–423.
- [49] D. Stadler and J. Beyerer, “Improving multiple pedestrian tracking by track management and occlusion handling,” in *Proceedings of the IEEE/CVF conference on computer vision and pattern recognition*, 2021, pp. 10 958–10 967.
- [50] S. Han, P. Huang, H. Wang, E. Yu, D. Liu, and X. Pan, “Mat: Motion-aware multi-object tracking,” *Neurocomputing*, vol. 476, pp. 75–86, 2022.
- [51] J. Cao, X. Weng, R. Khirodkar, J. Pang, and K. Kitani, “Observation-centric sort: Rethinking sort for robust multi-object tracking,” *arXiv preprint arXiv:2203.14360*, 2022.
- [52] P. Dendorfer, V. Yugay, A. Ošep, and L. Leal-Taixé, “Quo vadis: Is trajectory forecasting the key towards long-term multi-object tracking?” *Advances in neural information processing systems*, 2022.
- [53] P. Sun, J. Cao, Y. Jiang, R. Zhang, E. Xie, Z. Yuan, C. Wang, and P. Luo, “Transtrack: Multiple object tracking with transformer,” *arXiv preprint arXiv:2012.15460*, 2020.
- [54] Y. Xu, Y. Ban, G. Delorme, C. Gan, D. Rus, and X. Alameda-Pineda, “Transcenter: Transformers with dense representations for multiple-object tracking,” 2021.
- [55] F. Zeng, B. Dong, Y. Zhang, T. Wang, X. Zhang, and Y. Wei, “Motr: End-to-end multiple-object tracking with transformer,” in *European Conference on Computer Vision (ECCV)*, 2022.
- [56] N. Carion, F. Massa, G. Synnaeve, N. Usunier, A. Kirillov, and S. Zagoruyko, “End-to-end object detection with transformers,” in *European conference on computer vision*. Springer, 2020, pp. 213–229.
- [57] X. Zhou, T. Yin, V. Koltun, and P. Krähenbühl, “Global tracking transformers,” in *Proceedings of the IEEE/CVF Conference on Computer Vision and Pattern Recognition*, 2022, pp. 8771–8780.
- [58] E. Yu, Z. Li, S. Han, and H. Wang, “Relationtrack: Relation-aware multiple object tracking with decoupled representation,” *IEEE Transactions on Multimedia*, 2022.
- [59] G. Brasó and L. Leal-Taixé, “Learning a neural solver for multiple object tracking,” in *Proceedings of the IEEE/CVF conference on computer vision and pattern recognition*, 2020, pp. 6247–6257.
- [60] Y. Yuan, X. Weng, Y. Ou, and K. M. Kitani, “Agentformer: Agent-aware transformers for socio-temporal multi-agent forecasting,” in *Proceedings of the IEEE/CVF International Conference on Computer Vision*, 2021, pp. 9813–9823.
- [61] K. He, X. Zhang, S. Ren, and J. Sun, “Deep residual learning for image recognition,” in *Proceedings of the IEEE conference on computer vision and pattern recognition*, 2016, pp. 770–778.
- [62] J. L. Ba, J. R. Kiros, and G. E. Hinton, “Layer normalization,” *arXiv preprint arXiv:1607.06450*, 2016.
- [63] R. Girshick, “Fast r-cnn,” in *Proceedings of the IEEE international conference on computer vision*, 2015, pp. 1440–1448.
- [64] H. W. Kuhn, “The hungarian method for the assignment problem,” *Naval research logistics quarterly*, vol. 2, no. 1-2, pp. 83–97, 1955.
- [65] J. Luiten, A. Ošep, P. Dendorfer, P. Torr, A. Geiger, L. Leal-Taixé, and B. Leibe, “Hota: A higher order metric for evaluating multi-object tracking,” *International journal of computer vision*, vol. 129, no. 2, pp. 548–578, 2021.
- [66] E. Ristani and Solera, “Performance measures and a data set for multi-target, multi-camera tracking,” in *European conference on computer vision*. Springer, 2016, pp. 17–35.
- [67] E. Ristani, F. Solera, R. Zou, R. Cucchiara, and C. Tomasi, “Performance measures and a data set for multi-target, multi-camera tracking,” in *Computer Vision—ECCV 2016 Workshops: Amsterdam, The Netherlands, October 8-10 and 15-16, 2016, Proceedings, Part II*. Springer, 2016, pp. 17–35.
- [68] D. P. Kingma and J. Ba, “Adam: A method for stochastic optimization,” *arXiv preprint arXiv:1412.6980*, 2014.

- [69] J. Pang, L. Qiu, X. Li, H. Chen, Q. Li, T. Darrell, and F. Yu, “Quasi-dense similarity learning for multiple object tracking,” in *Proceedings of the IEEE/CVF conference on computer vision and pattern recognition*, 2021, pp. 164–173.
- [70] J. Wu, J. Cao, L. Song, Y. Wang, M. Yang, and J. Yuan, “Track to detect and segment: An online multi-object tracker,” in *Proceedings of the IEEE/CVF conference on computer vision and pattern recognition*, 2021, pp. 12 352–12 361.
- [71] C. Liang, Z. Zhang, X. Zhou, B. Li, S. Zhu, and W. Hu, “Rethinking the competition between detection and reid in multiobject tracking,” *IEEE Transactions on Image Processing*, vol. 31, pp. 3182–3196, 2022.
- [72] P. Tokmakov, J. Li, W. Burgard, and A. Gaidon, “Learning to track with object permanence,” in *Proceedings of the IEEE/CVF International Conference on Computer Vision*, 2021, pp. 10 860–10 869.